PAPER 57 – ANALYSIS AND SIMULATION OF A ROTOR FLUX-ORIENTED CONTROL SCHEME FOR A THREE PHASE INDUCTION MOTOR AT VARIABLE SPEED

G. A. Olarinoye

Department of Electrical Engineering, Ahmadu Bello University, Zaria, Kaduna, Nigeria.
*Email: baolarinoye@abu.edu.ng

ABSTRACT
The performance of induction motor drives under variable speed conditions can be improved by computing the optimum flux that guarantees minimum loss and therefore maximum efficiency in the motor. In this paper, a method to optimize the flux and thereby minimize the losses in a three-phase induction motor under variable speed conditions was developed. Mathematical models for the conventional rotor flux-oriented control scheme, total power loss as a function of rotor flux and optimum flux as a function of operating speed and load torque were analytically derived. A MATLAB/Simulink model of the proposed rotor flux optimization scheme was developed, as well, to verify the analyses set forth for a typical three-phase Induction Motor. The results of the proposed method were compared with those of the conventional rotor flux control method and direct torque control method in terms of loss reduction and efficiency for the same induction motor. The proposed rotor flux optimization scheme achieved significant improvements in efficiency and power loss compared to the conventional rotor flux control scheme. It also achieved a 5.01% improvement in efficiency compared to the optimized DTC control scheme at a speed of 250 rad/s for a load torque of 3Nm. At a lower speed of 150 rad/s, power loss was reduced by 17.2% while efficiency increased by 5.7% for the same load torque under the proposed scheme as compared to the optimized DTC scheme.

KEYWORDS: Induction motor, rotor flux, control, optimum, variable speed.

11. INTRODUCTION

Rotor flux-oriented control strategy allows precise and rapid control of the electromagnetic torque and hence speed in the three-phase induction machine. The torque control is accomplished by varying the stator current in such a way as to produce the amount of torque and speed commanded while at the same time keeping the rotor flux constant. The *d*-axis of the synchronously rotating *q*-*d* reference frame is aligned with the rotor flux. With this alignment, the *q*-component of the rotor flux is set to zero thereby producing what is referred to as the rotor flux-oriented control. The scheme uses the *q* and *d*-axis components of the stator current to control the rotor flux and maintain its proper orientation in the *q*-*d* reference frame. The rotor flux can be regulated in the desired torque and speed operating range to increase motor drive efficiency. By proper computation of the flux level in the motor, it is possible to minimize the losses in the motor. The copper and core losses account for the largest amount of losses in induction motor and therefore explains the interest to use them in the analysis proposed in this paper. To increase the motor drive efficiency, the flux must be reduced and balance obtained between copper and core losses. In this paper, Loss based model approach that determines the optimal flux for loss minimization is analysed and implemented in MATLAB/Simulink.
Sruthi *et al.* (2017) formulated a loss minimization algorithm for energy saving and efficiency improvement in induction motor drives. The input voltage and frequency were optimized to reduce total losses. Eseosa & Christian (2018), Nam & Uddin (2006) and Laroui, *et al*. (2021) presented various approaches to optimization control techniques to improve the efficient operation of induction motors. Aygun & Aktas (2018) implemented a direct torque control (DTC) technique combined with an online loss minimization model-based controller (LMC) to minimize the losses of an induction motor applied in an Electric Vehicle (EV). The objective of this paper is to develop a rotor flux optimization control model for an existing three-phase induction motor and simulate its performances in MATLAB/Simulink for loss minimization under variable speed conditions.

12. THEORETICAL ANALYSIS

The dynamic model of the induction motor in *d*-*q* coordinates established in a rotor flux-oriented reference frame is provided in equations (1) – (10) (Sharma, Parashar and Chandel, 2020; Olarinoye *et al*., 2022).

$$V_{qs} = R_s i_{qs} + \omega_e \lambda_{ds} + p\lambda_{qs} \quad (1)$$

$$V_{ds} = R_s i_{ds} - \omega_e \lambda_{qs} + p\lambda_{ds} \quad (2)$$
$$V'_{qr} = R'_r i'_{qr} + (\omega_e - \omega_r)\lambda'_{dr} + p\lambda'_{qr} \quad (3)$$
$$V'_{dr} = R'_r i'_{dr} - (\omega_e - \omega_r)\lambda'_{qr} + p\lambda'_{dr} \quad (4)$$
$$\lambda_{qs} = (L_{ms} + L_{ls})i_{qs} + L_{ms} i'_{qr} \quad (5)$$
$$\lambda_{ds} = (L_{ms} + L_{ls})i_{ds} + L_{ms} i'_{dr} \quad (6)$$
$$\lambda'_{qr} = L_{ms} i_{qs} + (L_{ms} + L'_{lr})i'_{qr} \quad (7)$$
$$\lambda'_{dr} = L_{ms} i_{ds} + (L_{ms} + L'_{lr})i'_{dr} \quad (8)$$
$$T_e = \frac{p}{2}\frac{L_{ms}}{L'_r}\left(\lambda'_{dr} i_{qs} - \lambda'_{qr} i_{qs}\right) \quad (9)$$
$$T_e = \frac{2j}{p} P\omega_r + T_L \quad (10)$$

V_{ds} and V_{qs}, V'_{dr} and V'_{qr} are the direct axes and quadrature axes stator and rotor voltages, and i_{ds}, i_{qs}, i'_{dr} and i'_{qr} are stator and rotor currents, λ_{ds}, λ_{qs}, λ'_{dr} and λ'_{qr} are stator and rotor flux respectively. R_s and R_r are stator and rotor resistances respectively. ω_e is stator frequency and ω_r is the rotor's electrical speed.

2.2 R**otor flux-oriented control scheme for the three-phase induction motor**

The rotor flux-oriented control is derived from the rotor dynamic equations of the three-phase induction machine in the synchronously rotating reference frame represented by equations (3)-(4) and (7)-(8). The set of equations that establish this control scheme is given as follows; (Olarinoye *et al*., 2022)

$$\lambda'_{qr} = 0 \quad (11)$$
$$\lambda'_r = \sqrt{\lambda'^2_{qr} + \lambda'^2_{dr}} \quad (12)$$
$$\lambda'_r = \lambda'_{dr}. \quad (13)$$
$$0 = R'_r l'_{qr} + (w_e - w_r)\lambda'_r \quad (14)$$
$$0 = R'_r l'_{dr} + \rho\lambda'_{dr} \quad (15)$$
$$\lambda'_r = L_m l'_{ds} + L_r l'_{dr} \quad (16)$$
$$0 = L_m l_{qs} + L_r l'_{qr} \quad (17)$$
$$\frac{\tau_r d\lambda'_r}{dt} + \lambda'_r = L_m l_{ds} \quad (18)$$
$$\tau_r = \frac{L_r}{R_r} \quad (19)$$
$$w_s = w_e - w_r = \frac{R'_r L_m l_{qs}}{L'_r \lambda'_r} \quad (20)$$
$$\theta_e = \int \omega_e \, dt = \int \left(\omega_r + \frac{R'_r L_m l_{qs}}{L'_r \lambda'_r}\right) dt \quad (21)$$
$$T_{em} = \frac{3P}{4}\frac{L_m}{L_r}\lambda'_r i'_{qs} \quad (22)$$

$L_r$and L_m are the self and mutual inductances of the rotor circuit. The rotor flux magnitude λ'_r and its phase angle, θ_e are estimated from equations (18) and (21) respectively.

13. METHODOLOGY

The loss model and therefore, the optimum flux expression are formulated from the equivalent circuit model of the three-phase induction motor shown in Figure 1. The following voltage, flux linkage and current equations can be obtained from Figure 1 as follows;

$$V_{qs} = r_s i'_{qs} + \mathrm{k}\omega_e \lambda_{ds} + kp\lambda_{qs} \quad (23)$$
$$V_{ds} = r_s i'_{ds} - \mathrm{k}\omega_e \lambda_{qs} + kp\lambda_{ds} \quad (24)$$
$$0 = r_r{}' i'_{qr} + (\omega_e - \omega_r)\lambda'_{dr} + p\lambda'_{qr} \quad (25)$$
$$0 = r_r{}' i'_{dr} - (\omega_e - \omega_r)\lambda'_{qr} + p\lambda'_{dr} \quad (26)$$
$$i_{cq} = i_{qs} - i'_{qs} \quad (27)$$
$$i_{cd} = i_{ds} - i'_{ds} \quad (28)$$
$$i_{cq} = \frac{V_{qs}}{kr_c} \quad (29)$$
$$i_{cd} = \frac{V_{ds}}{kr_c} \quad (30)$$

$$k = 1 + \frac{r_s}{r_c} \tag{31}$$

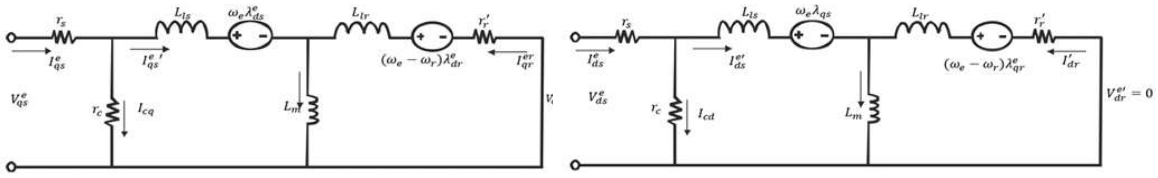

Figure 1: *q-d* equivalent circuit with core loss resistance

i_{cq} and i_{cd} are the currents flowing through the core loss branches of the *q* and *d* axes respectively. i'_{qs} and i'_{ds} are the torque currents responsible for producing electromagnetic torque in the motor as seen from the equivalent circuit. By applying equations (11) and (13) to the voltage equations (23) – (26), relationships between the applied stator currents and torque currents were obtained as follows;

$$\begin{bmatrix} i_{qs} \\ i_{ds} \end{bmatrix} = \begin{bmatrix} (1 + \frac{r_s}{kr_c}) & \frac{\omega_e L_s}{r_c} \\ -\frac{\omega_e L_x}{r_c} & (1 + \frac{r_s}{kr_c}) \end{bmatrix} \begin{bmatrix} i'_{qs} \\ i'_{ds} \end{bmatrix} \tag{32}$$

$$\begin{bmatrix} i'_{qs} \\ i'_{ds} \end{bmatrix} = \frac{1}{\left[1+\frac{r_s}{kr_c}\right]^2 + \frac{\omega_e^2 L_x L_s}{r_c^2}} \begin{bmatrix} (1 + \frac{r_s}{kr_c}) & -\frac{\omega_e L_s}{r_c} \\ \frac{\omega_e L_x}{r_c} & (1 + \frac{r_s}{kr_c}) \end{bmatrix} \begin{bmatrix} i_{qs} \\ i_{ds} \end{bmatrix} \tag{33}$$

The power loss model was formulated considering that the total electrical power loss is the sum of the copper and core losses in the motor. The expression of electrical power loss is obtained from the equivalent circuits as follows;

$$P_L = R_s\left(i_{qs}^2 + i_{ds}^2\right) + r_r'\left(i_{qr}^2 + i_{dr}^2\right) + r_c(i_{cq}^2 + i_{cd}^2) \tag{34}$$

A power loss model was derived by substituting current equations (29) – (33) into equation (34). It is given as follows;

$$\mathrm{P_L} = \frac{3}{2}\left[\frac{2\mathrm{T_e^2 L_r^2}}{\mathrm{k_t^2 L_m^2 \lambda_r^2}} + \frac{\mathrm{Z\lambda_r^2}}{\mathrm{L_m^2}} - \frac{\mathrm{r_r \lambda_r^2}}{\mathrm{L_r^2}} + \mathrm{kL_m^2}\left(\frac{\mathrm{r_r^2 + L_r^2 \omega_r^2}}{\mathrm{r_c L_r^4}}\right)\lambda_\mathrm{r}^2 - \ 2\mathrm{k}\lambda_\mathrm{r}^2\left(\frac{\mathrm{r r_r - \omega_e \omega_r L L_c}}{\mathrm{L_r^2 r_c}}\right) + \frac{2\mathrm{T_e}}{\mathrm{k_t r_c}}\left(\frac{\mathrm{k(\omega_e L r_r + \omega_r r L_r)}}{\mathrm{L_r}} + \mathrm{r_s \omega_e}\right)\right] \tag{35}$$

The optimum value of the rotor $\lambda_{r(opt)}$ flux for a given load torque and speed was obtained by differentiating equation (35) with respect to the rotor flux magnitude and equating the derivative to zero.

$$\lambda_{\mathrm{r(opt)}} = \sqrt{\frac{\mathrm{T_e L_r^3}}{\mathrm{k_t}}} \cdot \sqrt[4]{\frac{\mathrm{Z r_c}}{\mathrm{kL_m^2(\omega_r^2 L_m^2 L_r^2 + 2\omega_e \omega_r L L_r^3 + L_m^2 r_r^2) + Z L_r^4 r_c - r_r L_r^2 r_c L_m^2 - 2k r r_r L_r^2 L_m^2}}} \tag{36}$$

With equation (36), it is possible to minimize total electrical losses, $\mathrm{P_L}$ in the motor. For controller design, the stator voltages are expressed as a function of the *d* and *q*-axis currents and the rotor flux by applying equations (5) - (8), (11) and (13) to equations (23) and (24). The following expressions were obtained;

$$V_{qs} = Kr_s' i'_{qs} + KLpi'_{qs} + K\omega_e L i'_{ds} + K\frac{L_m}{L_r}\omega_r \lambda'_r \tag{39}$$

$$V_{ds} = Kr_s' i'_{ds} + KLpi'_{ds} - K\omega_e L i'_{qs} - K\frac{L_m}{L_r^2} R_r \lambda'_r \tag{40}$$

$$L = L_s\left(1 - \frac{{L_m}^2}{L_s L_r}\right) \tag{41}$$

$$r_s' = r_s + \frac{L_m^2 R_r}{L_r^2} \tag{42}$$

Equations (39) and (40) are first-order non-linear systems for which V_{qs} and V_{ds} are inputs and i'_{qs} and i'_{ds} are outputs. The voltage commands needed to give the desired currents, i'_{qs} and i'_{ds}, are obtained with a feedback-based solution using current controllers. The formulation for the controller gains was performed using equations (39) and (40). The proportional and integral gains, k_{pi} and k_{ii} for the stator current controller were derived as;

$$k_{pi} = KL2\zeta\omega_n - Kr_s' \tag{43}$$

$$k_{ii} = KL\omega_n^2 \tag{44}$$

ζ is the damping ratio and ω_n is the natural frequency. The speed control and rotor flux control loops provide the *d* and *q*-axis current commands respectively according to equations (18), (22) and (10). PI controllers were also employed for the speed and flux control loops. The speed controller gains are obtained as;

$$k_{pw} = 2\frac{J}{p}\omega_n \tag{45}$$

$$k_{iw} = \frac{J}{p}\omega_n^2 \quad (46)$$

Similarly, the flux controller gains are obtained as;

$$k_{pf} = \frac{\tau_r}{L_m} 2\omega_n - \frac{1}{L_m} \quad (47)$$

$$k_{if} = \frac{\tau_r}{L_m}\omega_n^2 \quad (48)$$

The supply voltages in the synchronous reference frame are then calculated based on the following equations;

$$V_{qs} = \sigma_{qs} + K(\omega_e L i'^e_{ds} + \frac{L_m}{L_r}\omega_r \lambda'^e_r) \quad (49)$$

$$V_{ds} = \sigma_{ds} - K\left(\frac{L_m R_r}{L_r^2}\lambda'^e_r + \omega_e L i'^e_{qs}\right) \quad (50)$$

Figure 2 shows the block diagram of the drive scheme for the three-phase induction machine. The analysis set forth was programmed for simulation and verification in MATLAB/Simulink.

14. RESULTS AND DISCUSSION

The motor parameters utilized to verify the effectiveness of the proposed scheme are provided in Table 1.

Table 1: Induction Motor Parameters.

S/N	Parameters		S/N	Parameters	
1	Voltage	400V	7	R_r	1.52Ω
2	Frequency	50HZ	8	r_c	13400Ω
3	Synchronous speed	3000rpm	9	$L_s = L_r$	0.2405H
4	No of poles	2	10	L_m	0.2323H
5	Power	3kW	11	J	0.0044kgm^2
6	R_s	1.795Ω	12		

The computed controller gains are provided in Table 2.

Table 2: Current, speed and flux controller gains

Controller	**Proportional gain**	**Integral gain**
q-axis current controller (k_i, k_p)	639.4058	6.3958e+06
d-axis current controller (k_i, k_p)	639.4058	6.3958e+06
Speed controller (k_i, k_p)	1.76	176
Flux controller (k_i, k_p)	268.1424	2.7245e+04

The loss minimization program was set to trigger at 2.5s. With the reference speed and load torque set to 250 rad/s and 3Nm respectively, the rated flux was computed as 1Wb. The rotor flux-oriented control scheme enables the variation of motor speed. To this end, the motor speed was ramped down from 250 rad/s to 150 rad/s and maintained between 4 and 5s of simulation time. Figures 3-5 show the performances of the motor under the proposed scheme at variable speeds.

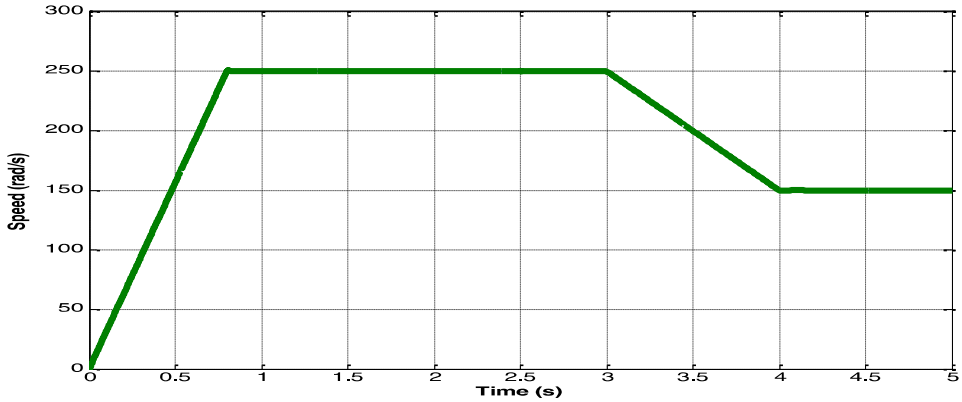

Figure 3: Variable speed profile of the induction motor

Figure 4 shows the plot of the rotor flux magnitude. It can be seen that the flux value is 1Wb until the proposed scheme is activated and the flux reduces significantly to its optimal value of 0.6357Wb for the given load torque.

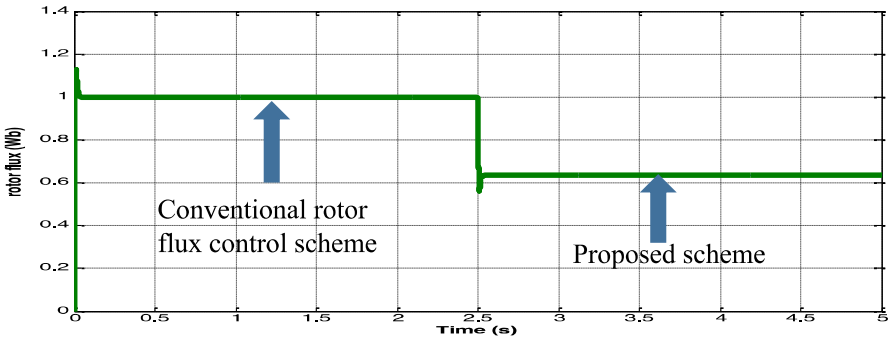

Figure 4: Rotor flux magnitude vs time

The total power loss is plotted in Figure 5. It can be seen that the conventional rotor flux control scheme produces a steady state power loss of 200W in the motor. The proposed scheme on the other hand, upon activation at a time of 2.5 s, produces a power loss of 108.04W in the same motor. The power loss further reduces to 83.645W because of the drop in speed. The total power loss therefore reduces by 22.6% and this implies that there is an opportunity to save power when the motor is driven at a lower speed.

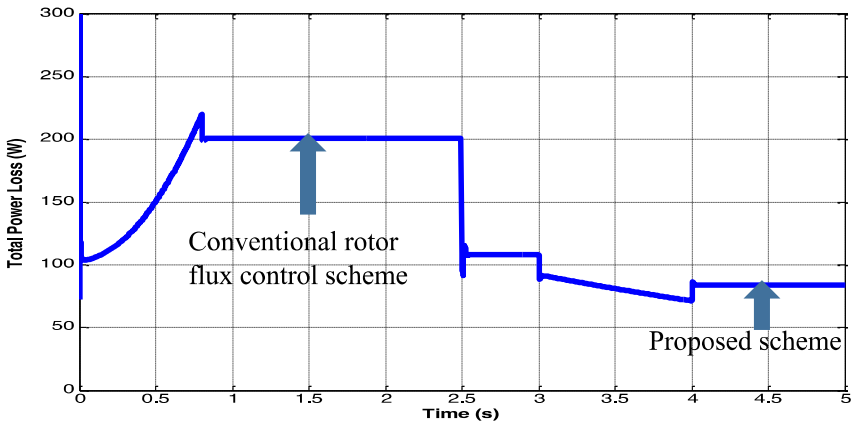

Figure 5: Total electric power loss under variable speed.

The efficiency of the motor is plotted in Figure 6. The motor efficiency rises from 78.9% for the conventional scheme to 87.41% for the proposed scheme at 250 rad/s as shown. It can also be seen to decrease to a value of 84.8% after the motor speed is dropped to 150 rad/s because the power output drops with speed. A table of comparison between these results and those obtained by Aygun and Aktas (2018) is provided in Table 2.

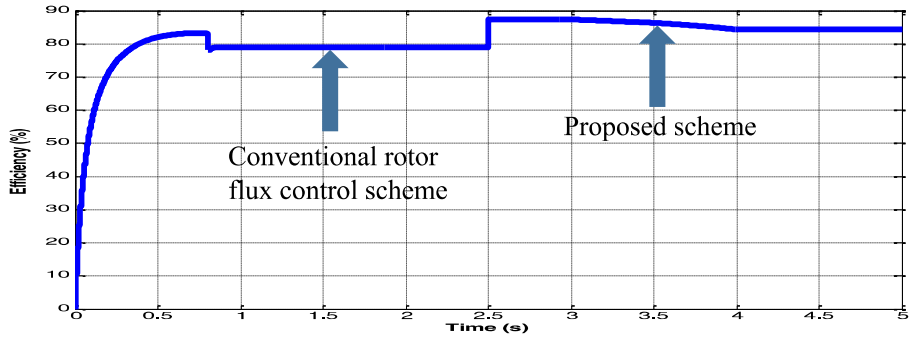

Figure 6: Efficiency of an induction motor under variable speed

Table 2: Comparison of results of the proposed rotor flux-oriented control scheme with those of the optimized DTC at variable speed

Scheme	Total power loss (W)	Efficiency (%)
Proposed scheme at 250 rad/s	108.04	87.41
Proposed scheme at 150 rad/s	83.645	84.8
Optimized DTC at 250 rad/s	166.28	82.4
Optimized DTC at 150 rad/s	101	79.1

Table 2 shows the superior performance of the proposed method at variable speed when compared with the performance of the optimized DTC method under the same operating conditions. At a lower speed of 150 rad/s, power loss reduces by 17.2% while efficiency is higher by 5.7% for a load torque of 3Nm under the proposed scheme as compared to the optimized DTC scheme developed in Aygun and Aktas (2018).

15. CONCLUSION

A rotor flux-oriented control model with optimization for a three-phase induction motor was analysed and simulated. The results obtained showed significant improvements over the conventional rotor flux control drive and the Direct torque control (DTC) drive of the same three-phase induction motor. A comparison of the conventional and proposed rotor flux-oriented control drive shows that when the reference speed was set to 250rad/s at a load torque of 3Nm, the rotor flux reduced from a rated value of 1Wb to an optimal value of 0.6357Wb thereby leading to a significant reduction of the total power loss from 200W to 108.04W and a consequential increase in efficiency from 78.9% to 87.41%. With the proposed drive scheme operating at variable speed mode in which motor speed was ramped down from 250rad/s to 150rad/s at a load torque of 3Nm, power loss is observed to further reduce significantly to 83.645W giving a reduction of 22.6%. A comparison between the results obtained and those obtained by Aigun and Aktas (2018) shows that the proposed rotor flux optimization control scheme is superior to the optimized Direct Torque Control (DTC) scheme for the same motor parameters. At a speed of 150 rad/s, power loss was reduced by 17.2% while efficiency increased by 5.7% for the same load torque under the proposed scheme as compared to the optimized DTC scheme.

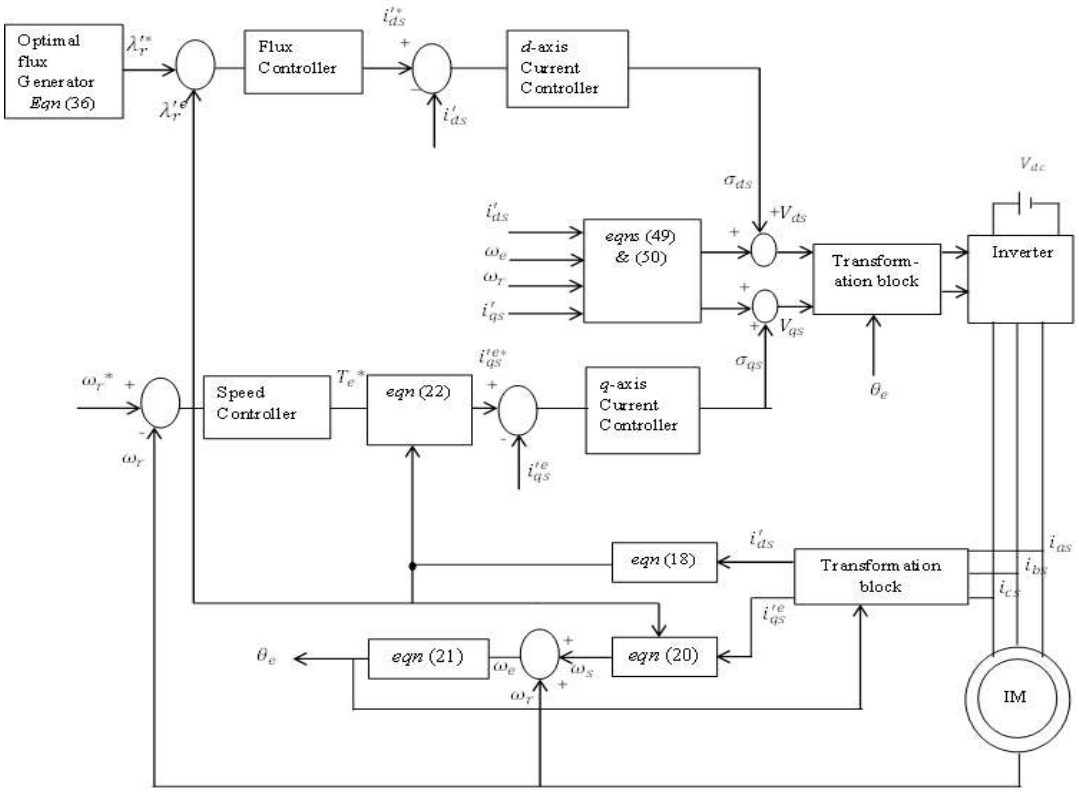

Figure 2: Block diagram of three phase induction motor drive scheme

REFERENCES

Aygun, H. and Aktas, M. (2018). A novel DTC method with efficiency improvement of IM for EV applications. Engineering, Technology & Applied Science Research, 8(5), 3456-3462.

Eseosa, O. and Christian, A. (2018). Energy Efficiency Optimization of Three-Phase Induction Motor Drives for Industrial Applications. Int. J. Eng. Appl. Sci, *5*(8).

Laroui, M.; Nour, B.; Moungla, H.; Cherif, M. A.; Afifi, H. and Guizani, M. (2021). Edge and fog computing for IoT: A survey on current research activities & future directions. Computer Communications, 180, 210-231.

Nam, S. W. and Uddin, M. N. (2006). Model-based loss minimization control of an induction motor drive. In IEEE International Symposium on Industrial Electronics. 3(1), pp. 2367-2372). IEEE.

Olarinoye, G. A.; Akorede, M.F and Akinropo, C. D (2022). Design and Simulation of a Three-Phase Induction Motor Speed Control System. FUOYE Journal of Engineering and Technology. Federal University Oye-Ekiti, Nigeria. 7(1), pp. 39 – 46.

Sharma, G.; Parashar, D. and Chandel, A. (2020). Analysis of Dynamic Model of Three Phase Induction Motor with MATLAB/SIMULINK. International Conference on Advances in Computing, Communication & Materials (ICACCM), Dehradun, India, pp. 51-58. IEEE.

Sruthi, M. P.; Nagamani, C. and Ilango, G. S. (2017). An improved algorithm for direct computation of optimal voltage and frequency for induction motors. Engineering Science and Technology, an international journal, 20(5), 1439-1449.